



Research Papers

Cercospora leaf spot of olive in Uruguay

Citation: P. Lombardo, C. Leoni, S. Alaniz, P. Mondino (2023) Cercospora leaf spot of olive in Uruguay. *Phytopathologia Mediterranea* 62(3): 413-426. doi: 10.36253/phyto-14675

Accepted: November 7, 2023

Published: December 30, 2023

Copyright: ©2023 P. Lombardo, C. Leoni, S. Alaniz, P. Mondino. This is an open access, peer-reviewed article published by Firenze University Press (<http://www.fupress.com/pm>) and distributed under the terms of the Creative Commons Attribution License, which permits unrestricted use, distribution, and reproduction in any medium, provided the original author and source are credited.

Data Availability Statement: All relevant data are within the paper and its Supporting Information files.

Competing Interests: The Author(s) declare(s) no conflict of interest.

Editor: Lizel Mostert, Faculty of AgriSciences, Stellenbosch, South Africa.

ORCID:

PL: 0000-0002-6711-6556
CL: 0000-0002-3891-564X
SA: 0000-0002-6530-7279
PM: 0000-0002-4494-5271

PAMELA LOMBARDO^{1,*}, CAROLINA LEONI², SANDRA ALANIZ³, PEDRO MONDINO³

¹ *Departamento de Ciencias Biológicas, CENUR Litoral Norte, Universidad de la República, Gral. Rivera 1350 CP 50000, Salto, Uruguay*

² *Unidad de Protección Vegetal, INIA Las Brujas, Ruta 48 km10, Rincón del Colorado, CP 90100, Canelones, Uruguay*

³ *Departamento de Protección Vegetal, Facultad de Agronomía, Universidad de la República, Av. Garzón 780 CP 12900, Montevideo, Uruguay*

*Corresponding author. E-mail: palomba@fagro.edu.uy

Summary. Cercospora Leaf Spot (CLS) of olive is an important fungal disease in Uruguay, causing severe early defoliation. Fungal isolates were obtained from olive leaves with typical CLS symptoms from Uruguayan orchards. The isolates were identified based on phenotypic characteristics and DNA sequence analyses. Infection processes under field conditions were characterized. Phylogenetic analyses confirmed that *Pseudocercospora cladosporioides* is the causal agent of CLS in Uruguay. Three colony morphologies were observed for isolates growing on potato dextrose agar. Mean conidium length ranged from 65.7 to 101.8 µm, and widths from 4.3 to 5.0 µm. Mean optimum growth temperature was 21.5°C (range 19.2 to 24.8°C). Under field conditions, initial CLS symptoms on leaves were observed 5 months after inoculation of cv. Arbequina plants, confirming the disease's lengthy incubation period. This study shows that CLS as one of the most prevalent and destructive olive diseases in Uruguay, and emphasizes the importance of further research to develop efficient management of this disease.

Keywords. 'Arbequina', etiology, *Olea europaea*, *Pseudocercospora cladosporioides*.

INTRODUCTION

Olive (*Olea europaea* subsp. *europaea* L.) is an important fruit crop in Uruguay, covering around 5,900 ha. The most commonly planted olive cultivars are Arbequina (47%), Coratina (21%), Picual (11%), and Frantoio (10%) (MGAP-DIEA, 2020). The Uruguayan climate is characterized by frequent high humidity days and abundant rainfall, favouring development of fungal leaf and fruit diseases of olive (Conde-Innamorato *et al.*, 2019).

Cercospora leaf spot (CLS) is an endemic and severe olive disease (Del Moral and Medina, 1985) that is widely distributed in most olive-growing areas, causing severe losses during wet years in susceptible cultivars (Trapero *et al.*, 2017). However, in the Mediterranean basin region where most olive production is concentrated, little research has focused on this disease. In that region, CLS is considered as less severe than other olive diseases, such as anthracnose or olive scab (Garrido *et al.*, 2022).

CLS causes severe “early leaf drop” defoliation of olive trees. Affected leaves have diffuse and chlorotic areas on the adaxial surfaces which evolve necrotically, and leaden-grey areas on the abaxial surfaces due to the presence of conidia. Host petioles, peduncles (Ávila *et al.*, 2004; Agustí-Brisach *et al.*, 2016), and young twigs can also be affected, where blackened spots of different shapes and sizes can be observed (Pappas, 1993; Nigro and Ferrara, 2011). Olive fruit can also be affected, and symptoms vary from brown, sunken areas of a few millimetres diam. on green olives to more extensive areas with pale yellow haloes on ripening fruit. Severe symptoms cause decreases in fruit quality and oil production, due to fruit drop, increased acidity, and reduced oil yields (Trapero *et al.*, 2017; Avila *et al.*, 2020, Romero *et al.*, 2020).

The causal agent of CLS is the fungus *Pseudocercospora cladosporioides*, which is characterized by slow growth in culture media and little or no production of conidia (Pappas, 1993; Ávila *et al.*, 2004, 2005, 2020; Nigro and Ferrara, 2011). Conidia of the fungus are produced in dark brown stromatic conidiomata, which arise in clusters through the host stomata or directly through the epidermis on the underside of infected leaves (Ávila *et al.*, 2004). Conidia are pale brown, straight or slightly curved, rounded at the apices and truncated at the bases, with variable dimensions and numbers of septa (Sarasola, 1951; Del Moral and Medina, 1985; McKenzie, 1990; Braun, 1993; Ávila *et al.*, 2004; Sergeeva *et al.*, 2008; Nigro and Ferrara, 2011). Little is known of the CLS disease cycle, except that the main inoculum source is affected leaves that remain attached to tree, and that the disease incubation period is long (up to 11 months) (Ávila *et al.*, 2004; Sergeeva and Spooner-Hart, 2009; Agustí-Brisach *et al.*, 2016; Trapero *et al.*, 2017; Ávila *et al.*, 2020).

In Uruguay, Conde-Innamorato *et al.* (2013) found that CLS was one of the main foliar diseases affecting olive trees. However, farmers often lack awareness of this disease mistaking CLS for other foliar diseases such as olive scab or anthracnose, as well as symptoms caused by abiotic factors. Developing local knowledge of CLS is urgent to elucidate aspects of the disease that facilitate understanding the interactions between host plants, the pathogen, and the environment, and to develop effective control strategies. For this reason, the research outlined in this paper aimed to characterize the causal agent of CLS of olive in Uruguay using morphological and molecular analyses, and to characterize the infections process under field conditions.

MATERIALS AND METHODS

Field symptoms and fungal isolates

Between 2017 and 2018, a survey was conducted in 18 olive orchards situated in six departments located in the north (Salto), south (Colonia, Canelones, and Montevideo) and east (Maldonado and Rocha) of Uruguay (Table 1). The cultivars sampled were Arbequina, Arbosana, Coratina, Leccino, Manzanilla de Sevilla, Pendolino, Picholine, and Seggianese. In each orchard, symptoms attributable to CLS were carefully observed, and five to ten leaves with typical CLS symptoms were collected from different trees and used for pathogen isolations. From each leaf, the sporulating lesion was hydrated with 300 µL of sterile distilled water (SDW), and 100 µL of the conidium suspension were dispersed in each of 90 mm diam. Petri plates containing water agar (WA) amended with 0.4 g L⁻¹ of streptomycin sulphate (Sigma-Aldrich). After incubation for 24 h at 20°C in darkness, germinated conidia were transferred to a Potato Dextrose Agar (PDA, Oxoid Ltd.) and maintained under the same incubation conditions. A single monocolonial isolate was selected from each leaf sample.

The isolates were conserved in 15% glycerol at -80°C, and deposited at the fungal culture collection of the Department of Plant Protection, Faculty of Agronomy, University of the Republic, Uruguay.

Morphological characterization of isolates

Monosporic isolates were grown on PDA at 20°C, in darkness. After 30 d, the isolates were grouped in morphotypes according to colony appearance, shape, and colour. Monosporic isolates growing on Cornmeal Agar (CMA) in the same conditions were used for conidium characterization. Lengths, widths, and the numbers of septa from 20 conidia per isolate were assessed using a Dino Capture 2.0 digital imaging camera (Dino-Eye AM4023X) on an Eclipse E100Led microscope (Nikon Corp.) at ×400 magnification. Data of conidium lengths, widths, length/width ratios, and numbers of septa were subjected to analysis of variance (ANOVA) and Tukey's test (at $P = 0.05$) was used to compare the mean conidium values. These analyses were conducted using the RStudio v. 2023.06.1-524 program (<https://dailies.rstudio.com/version/2023.06.1+524/>).

Effects of temperature on isolate mycelium growth

Agar plugs (5 mm diam.) from the outer edges of 15-d-old cultures of isolates were transferred to the cen-

Table 1. Location details and Genbank accession numbers for Uruguayan *Pseudocercospora cladosporioides* isolates obtained from olive leaves, and identified in this study.

Isolate	Orchard	Cultivar ^a	Department, Locality	Morphotype ^b	GenBank Accession No.		
					ACT	CAL	ITS
E07	1	Arbequina	Salto, Olivares Salteños	a	ON442427	ON442509	ON442468
E10	1	Arbequina	Salto, Olivares Salteños	a	ON442428	ON442510	ON442469
E12	2	Arbequina	Salto, Olivares Salteños	a	ON442429	ON442511	ON442470
E15	2	Arbequina	Salto, Olivares Salteños	a	ON442430	ON442512	ON442471
E19	3	n/d	Salto, Punta de Valentín	c	ON442431	ON442513	ON442472
E20	3	n/d	Salto, Punta de Valentín	a	ON442432	ON442514	ON442473
E23	3	n/d	Salto, Punta de Valentín,	a	ON442433	ON442515	ON442474
E25	4	n/d	Salto, Punta de Valentín,	a	ON442434	ON442516	ON442475
E27	4	n/d	Salto, Punta de Valentín,	a	ON442435	ON442517	ON442476
E29	4	n/d	Salto, Punta de Valentín,	a	ON442436	ON442518	ON442477
E31	5	Arbequina	Rocha, Nuevo Manantiales	a	ON442437	ON442519	ON442478
E33	5	Arbequina	Rocha, Nuevo Manantiales	a	ON442438	ON442520	ON442479
E35	6	Coratina	Rocha, Nuevo Manantiales	a	ON442439	ON442521	ON442480
E37	6	Coratina	Rocha, Nuevo Manantiales	a	ON442440	ON442522	ON442481
E39	6	Coratina	Rocha, Nuevo Manantiales	b	ON442441	ON442523	ON442482
E40	6	Coratina	Rocha, Nuevo Manantiales	c	ON442442	ON442524	ON442483
E43	7	Manzanilla	Maldonado, Agroland	a	ON442443	ON442525	ON442484
E48	8	Leccino	Maldonado, Agroland	c	ON442444	ON442526	ON442485
E49	9	Coratina	Maldonado, Agroland	a	ON442445	ON442527	ON442486
E50	9	Coratina	Maldonado, Agroland	a	ON442446	ON442528	ON442487
E51	9	Coratina	Maldonado, Agroland	a	ON442447	ON442529	ON442488
E52	9	Coratina	Maldonado, Agroland	a	ON442448	ON442530	ON442489
E53	10	Arbequina	Maldonado, Agroland	a	ON442449	ON442531	ON442490
E58	11	Arbequina	Montevideo, ARU	a	ON442450	ON442532	ON442491
E59	11	Arbequina	Montevideo, ARU	c	ON442451	ON442533	ON442492
E60	11	Arbequina	Montevideo, ARU	a	ON442452	ON442534	ON442493
E66	12	Pendolino	Montevideo, ARU	a	ON442453	ON442535	ON442494
E68	12	Pendolino	Montevideo, ARU	a	ON442454	ON442536	ON442495
E69	12	Pendolino	Montevideo, ARU	a	ON442455	ON442537	ON442496
E70	13	Leccino	Canelones, INIA Las Brujas	b	ON442456	ON442538	ON442497
E71	13	Leccino	Canelones, INIA Las Brujas	b	ON442457	ON442539	ON442498
E72	14	Picholine	Canelones, INIA Las Brujas	a	ON442458	ON442540	ON442499
E73	15	Seggianese	Canelones, INIA Las Brujas	a	ON442459	ON442541	ON442500
E74	15	Seggianese	Canelones, INIA Las Brujas	b	ON442460	ON442542	ON442501
E76	16	n/d	Montevideo, FAgro	a	ON442461	ON442543	ON442502
E77	16	n/d	Montevideo, FAgro	a	ON442462	ON442544	ON442503
E78	17	Arbequina	Colonia, San Pedro	a	ON442463	ON442545	ON442504
E79	17	Arbequina	Colonia, San Pedro	c	ON442464	ON442546	ON442505
E82	18	Arbosana	Colonia, Astilleros,	a	ON442465	ON442547	ON442506
E83	18	Arbosana	Colonia, Astilleros	a	ON442466	ON442548	ON442507
E85	15	Seggianese	Canelones, INIA Las Brujas	a	ON442467	ON442549	ON442508

^a n/d: not determined^b Morphotype: a, grey and rough; b, whitish and rough; c, grey olivaceous and smooth.

tres of the fresh PDA plates. The plates were then incubated in darkness at different temperatures from 0°C to 35°C at 5°C increments. For each combination of isolate

and temperature, three replicates plates were used, and the experiment was performed twice. After 30 d, each colony diameter was measured along two perpendicular

Table 2. Details of primers used in this study for amplification and sequencing.

Locus	Primer	Sequence (5'-3')	Orientation	Annealing	Reference
ITS	ITS1	TCCGTAGGTGAACCTGCGG	Forward	57°C for 30 s	White <i>et al.</i> (1990)
	ITS4	TCCTCCGCTTATTGATATGC	Reverse		
ACT	ACT-512F	ATGTGCAAGGCCGGTTTCGC	Forward	52°C for 30 s	Carbone and Kohn (1999)
	ACT-783R	TACGAGTCCTTCTGGCCCAT	Reverse		
CAL	CAL-228F	GAGTTCAAGGAGGCCTTCTCCC	Forward	52°C for 30 s	Carbone and Kohn (1999)
	CAL-737R	CATCTTTCTGGCCATCATGG	Reverse		

axes, using a digital calliper (IP54; Truper Tools). These colony dimensions were averaged, and the radial growing rate (mm day⁻¹) was calculated.

To examine fluctuations in mycelial growth rates across different temperatures for each isolate, a non-linear data adjustment method was employed, using the Generalized Analytis Beta model (Hau and Kranz, 1990; López-Moral *et al.*, 2017). Subsequently, the optimum growth temperature (T_{opt}) was determined using the formula $T_{opt} = [(a \times T_{max}) + (b \times T_{min})] / (a + b)$ and the corresponding maximum growth rate (MGR) was calculated using the equation $Y = d \times (T - T_{min})^a \times (T_{max} - T)^b$. Data analyses were conducted using Statistix 10 (Analytical Software, 2013). Ten representative isolates were selected according to geographic origin, optimum growth temperature, and daily radial growth rate at the optimum temperature, according to non-linear model results, and subjected to ANOVA analysis. Tukey's test (at $P = 0.05$) was used to compare the mean growth rates. These analyses were carried out using the RStudio v. 2023.06.1-524 program.

Molecular characterization of isolates

DNA extraction, PCR analysis and sequencing

DNA was extracted from the mycelium of each monospore isolate following the protocol of Paolucci *et al.* (1999). Three genomic regions of each isolate were amplified, including the ITS region (ITS), using ITS1/ITS4 primers (White *et al.*, 1990), portions of actin (ACT), using ACT-512F/ACT-783R primers (Carbone and Kohn 1999), and calmodulin (CAL), using CAL-228F/CAL-737R primers (Carbone and Kohn 1999) (Table 2).

Each PCR reaction contained 1× PCR buffer, 2.5 mM MgCl₂, 0.4 mM of each dNTP, 0.4 μM of each primer, 0.5 U of DNA polymerase (Bioron), and 1 μL of template DNA. The PCR reactions were each adjusted to a final volume of 20 μL with MQ water. The amplifications were carried out on a MultiGene™ Mini thermal

cycler (Labnet International Inc.). The PCR program consisted on an initial step of 94°C for 5 min, followed by 35 cycles of denaturation at 94°C for 30 s, annealing at 57°C for ITS, and 52°C for ACT and CAL for 30 s, and elongation at 72°C for 45 s. The final extension was at 72°C for 10 min. PCR products were analyzed on 1.5% agarose gels stained with GelRed™, and were visualized in a transilluminator under UV light. A GeneRuler 100-bp DNA ladder plus (Thermo) was used as the molecular weight marker. PCR products were purified and sequenced at the Pasteur Institute, Montevideo, Uruguay.

Phylogenetic analyses

The sequences of each gene region were aligned using ClustalW, available within the MEGA v. 11.0.11 program (Tamura *et al.*, 2021). The sequences were compared with those deposited in NCBI GenBank nucleotide database (www.ncbi.nlm.nih.gov) using the BLAST source. Sequences of phylogenetically related species of *P. cladosporioides* (including the ex-epitype, CBS 117482) of the *Pseudocercospora* phylogenetic analysis Clade 14 (Crous *et al.*, 2013) were obtained from GenBank and incorporated into the alignments (Table 3).

Phylogenetic analyses were carried out separately for each ITS, ACT, and CAL region, and a multi-locus alignment was built using Concatenate Sequence Alignments available within the MEGA v. 11.0.11 program. Phylogenetic trees were constructed using Bayesian Inference (BI) with the MrBayes v. 3.2.7 program, and Maximum Likelihood (ML) with the RAXML v. 8.2.12 program, implemented in CIPRES Science Gateway v. 3.3 (<http://www.phylo.org/>). For BI phylogenetic analyses, the best-fit model of each gene region in each genus was selected, according to the corrected Akaike information criteria (cAIC) in MEGA v. 11.0.11, and Jukes Cantor (JC) resulted as the best model for the three gene regions. Four Marko Chain Monte Carlo (MCMC) chains were run simultaneously starting from a random

Table 3. GenBank sequences used in this study for phylogenetic analyses of representative fungal isolates.

Species ^a	Strain ^{ab}	Host	Origin country	Collector	GenBank Accession No. ^c		
					ITS	ACT	CAL
<i>Cercospora sojina</i>	CBS 132615 = CPC 11353	<i>Glycine soja</i>	South Korea	H.D. Shin	JX143659	JX143173	JX142927
<i>Pseudocercospora araliae</i>	CPC 10154	<i>Aralia elata</i>	South Korea	H.D. Shin	GU269652	GU320360	-
<i>P. araliae</i>	MUCC 873	<i>Aralia elata</i>	Japan	T. Kobayashi and C. Nakashima	GU269653	GU320361	-
<i>P. balsaminiae</i>	CBS 131882 = CPC 10044	<i>Impatiens textoriana</i>	South Korea	H.D. Shin	GU269660	GU320367	-
<i>P. boehmeriigena</i>	CPC 2524 = COAD 1562	<i>Bohemia nivea</i>	Brazil	R.W.Barreto	KT290152	KT313507	-
<i>P. cladosporioides</i>	CBS 113866	<i>Olea europaea</i>	Spain	A. Ávila et al.	AY438252	AY438244	AY438261
<i>P. cladosporioides</i>	CBS 113867	<i>Olea europaea</i>	Spain	A. Ávila et al.	AY438254	AY438246	AY438263
<i>P. cladosporioides</i>	CBS 114079	<i>Olea europaea</i>	Spain	A. Ávila et al.	AY438249	AY438241	AY438258
<i>P. cladosporioides</i>	CBS 117482 = CPC 10913	<i>Olea europaea</i>	Tunisia	P.W. Crous	GU269678	GU320383	DQ008124
<i>P. crocea</i>	CBS 126004 = CPC 11668	<i>Pilea hamaoi</i>	South Korea	H.D. Shin	GU269792	GU320493	-
<i>P. dendrobbii</i>	MUCC.596	<i>Dendrobium</i> sp.	Japan	C. Nakashima and K. Motohashi	GU269696	GU320401	-
<i>P. dianellae</i>	CBS 117746	<i>Dianella caeruleae</i>	New Zealand	C.F. Hill	GU269695	GU320400	-
<i>P. eucalyptorum</i>	CBS 110777 = CPC 16 = CMW 5228	<i>Eucalyptus nitens</i>	South Africa	P.W. Crous	AF309598	KF903406	KF902621
<i>P. eucalyptorum</i>	CPC 12406 = CBS 132029	<i>Eucalyptus globulus</i>	Australia	I. Smith	GU269793	GU320494	KF902616
<i>P. gracilis</i>	CBS 111189 = CPC 1315	<i>Eucalyptus urophylla</i>	Indonesia	M.J. Wingfield	DQ302960	JX902137	JX901572
<i>P. gracilis</i>	CBS 242-94 = CPC 729	<i>Eucalyptus urophylla</i>	Indonesia	P.W. Crous	DQ267582	DQ147616	-
<i>P. humulicola</i>	CBS 131585 = CPC 11358	<i>Humulus scandens</i>	South Korea	H.D. Shin	GU269723	GU320427	-
<i>P. humulicola</i>	CBS 131883 = CPC 10049	<i>Humulus scandens</i>	South Korea	H.D. Shin	GU269724	JQ325018	-
<i>P. jussiaeae</i>	CBS 132117 = CPC 14625	<i>Ludwigia prostrata</i>	South Korea	H.D. Shin	JQ324977	JQ325020	-
<i>P. lythri</i>	CBS 132115 = CPC 14588	<i>Lythrum salicaria</i>	South Korea	H.D. Shin	GU269742	GU320444	-
<i>P. lythri</i>	MUCC.865	<i>Lythrum salicaria</i>	Japan	I. Araki and M. Harada	GU269743	GU320445	-
<i>P. nephrolepidis</i>	CBS 119121	<i>Nephrolepis auriculata</i>	Taiwan	R. Kirschner	GU269751	GU320453	-
<i>P. plectranthi</i>	CBS 131586 = CPC 11462	<i>Plectranthus</i> sp.	South Korea	H.D. Shin	GU269791	GU320492	-
<i>P. pouzolziae</i>	CBS 122280	<i>Gonostegia hirta</i>	Taiwan	R. Kirschner	GU269761	GU320462	-
<i>P. profusa</i>	CBS 132306 = CPC 10055	<i>Acalypha australis</i>	South Korea	H.D. Shin	GU269762	GU320463	-
<i>P. profusa</i>	CPC 10042	<i>Acalypha australis</i>	South Korea	H.D. Shin	GU269787	GU320488	-
<i>P. rhabdothamni</i>	CBS 114872	<i>Rhabdothamnus solandri</i>	New Zealand	M. Fletcher	GU269768	GU320471	-
<i>P. robusta</i>	CBS 111175 = CPC 1269 = CMW 5151	<i>Eucalyptus robur</i>	Malaysia	M.J. Wingfield	AY309597	DQ147617	JX901579
<i>P. rumohrae</i>	CBS 117747	<i>Marattia salicina</i>	New Zealand	C.F. Hill	GU269774	GU320477	-
<i>Pseudocercospora</i> sp.	CPC 10058	<i>Potentilla kleiniana</i>	South Korea	H.D. Shin	JQ324979	JQ325022	-

^a Ex-epitype or holotype species and strain are indicated in bold font.^b CBS: Culture collection of the Westerdijk Fungal Biodiversity Institute, Utrecht, The Netherlands; CMW: Culture collection of the Forestry and Agricultural Biotechnology Institute (FABI) of the University of Pretoria, Pretoria, South Africa; COAD: Coleção Octavio de Almeida Drummond, housed at the Universidade Federal de Viçosa, Viçosa, Brazil; CPC: Culture collection of Pedro Crous, housed at the Westerdijk Institute; MUCC (in TSU): Culture Collection, Laboratory of Plant Pathology, Mie University, Tsu, Mie Prefecture, Japan.^c ITS: internal transcribed spacers; ACT: actin; CAL: calmodulin.

tree to 10 million generations. Trees were sampled every 1000 generations, and the first 2500 were discarded as the burn-in phase of each analysis. Posterior probabilities were determined from a majority-rule consensus tree generated with the remaining 7500 trees. For the ML analyses, a Generalized Time-Reversible with Gamma correction (GTR + GAMMA) nucleotide substitution model and 1000 bootstrap iterations were indicated. The other parameters were used as default settings. Sequences generated in this research were deposited in the GenBank (Table 1).

Characterization of infection under field conditions

To determine the period between inoculation and the onset of visible symptoms, field inoculations were carried out. Two experiments were carried out in 2021, one during autumn, the other in spring. The experiments were conducted on 15-year-old cv. Arbequina olive trees in an experimental orchard at the INIA Las Brujas Agricultural Research Station, Canelones, Uruguay (34°40'S, 56°20'W).

Inoculum used was from naturally infected olive leaves, following the methods outlined by Ávila *et al.* (2020). The inoculum was collected from two orchards situated in Rincón del Colorado, Canelones, one of which contained 'Frantoio' olive trees and the other contained cv. Arbequina trees. To obtain each conidium suspension, 150 leaves with sporulating lesions were placed in an Erlenmeyer flask containing 100 mL of sterile distilled water (SDW) plus a drop of Tween 20. The flask was then shaken for 1 h to dislodge the conidia, and the resulting suspension was filtered through sterile gauze. The concentration of conidia was then adjusted to 1.5×10^5 conidia mL⁻¹, using haemocytometer assessments. To check conidium germination, an aliquot from each suspension was plated on water agar, and germination was evaluated after 24 h. Conidium suspensions with germination greater than 75% were used for inoculations.

Three 15-year-old cv. Arbequina trees were randomly chosen from the experimental orchard. Within each tree, four new shoots were selected, positioned, respectively, in the north (N), south (S), east (E), or west (W) quadrants of the tree, with each shoot containing approx. ten leaves. The shoots were sprayed with conidium suspension until runoff. To establish the baseline level of latent infections at the beginning of the experiment, an additional four shoots in each of the same trees and quadrants were inoculated with SDW plus Tween 20 as experimental controls. Each individual shoot was subsequently enclosed within a white non-textile cloth bag

until the conclusion of the experiment, to prevent further natural infections caused by *P. cladosporioides*.

Monthly evaluations were carried out during 1 year after inoculations, to determine the presence or absence of symptoms related to CLS on each leaf of the inoculated and control treatments. Presence of characteristic *P. cladosporioides* conidia was also assessed using microscope examinations.

RESULTS

Field symptoms and fungal isolates

Typical symptoms of CLS were observed in all the surveyed commercial olive groves. Leaf spots were observed mainly in adult leaves in the middle to lower parts of each tree. On the upper surfaces of the affected leaves, the spots were greenish-yellow to yellow with diffuse edges (Figure 1 a), and some leaves completely yellow or with necrotic areas. On the undersides of the leaves, grey areas of fungal sporulation were observed (Figure 1 b), consisting of typical conidiophores and conidia of *P. cladosporioides* (Figure 1, f and g). Fungal sporulation was often observed before symptoms, especially in Frantoio and Picual cultivars, and severe defoliation was often present (Figure 1 c).

No symptoms were observed on olive fruit during the two years of survey, so no isolates were derived from fruit. Only during August 2022 in one southern orchard (Canelones department) were typical symptoms of CLS observed on unharvested 'Coratina' olives 5 months after conventional harvest. Affected olives had irregular purple or light brown spots that progressed into depressed greyish-brown areas. A binocular magnifying glass and microscope examinations (Figure 1, d and e) showed typical conidiomata and conidia of *P. cladosporioides*.

A total of 41 monosporic isolates were obtained from leaves exhibiting CLS symptoms, sourced from the 18 olive orchards, as indicated in Table 1.

Morphological characterization of isolates

The isolates exhibited typical morphological characteristics of *P. cladosporioides*. After 15 d incubation at 20°C, the colonies had smooth and well-defined margins, and moderate aerial mycelium. The colonies were smoke-grey to pale olivaceous-grey, with iron-grey reverse sides.

The colonies were of three morphotypes, based on colour and appearance. Thirty-two isolates were of morphotype a (Figure 2 a), with grey rough colonies with

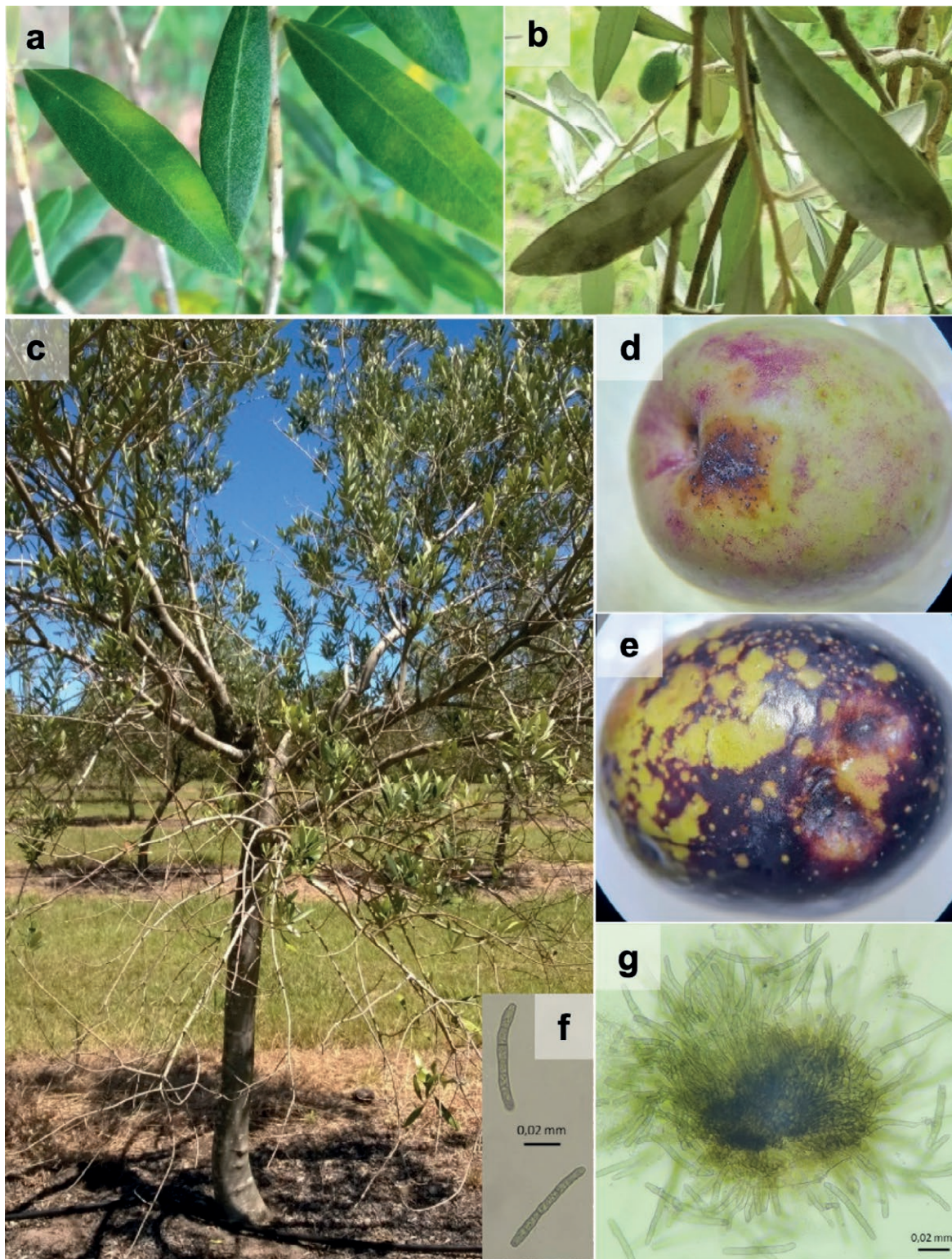


Figure 1. Symptoms of CLS on the olive tree caused by *Pseudocercospora cladosporioides*. a: chlorotic spots on the adaxial surface of the leaves and b: leaden grey areas on the abaxial side due to fructifications of the fungus; c: olive trees with severe defoliation; d and e: fruits with CLS symptoms and reproductive structures of the fungus; f: conidia and g: conidioma of *Ps. cladosporioides*.

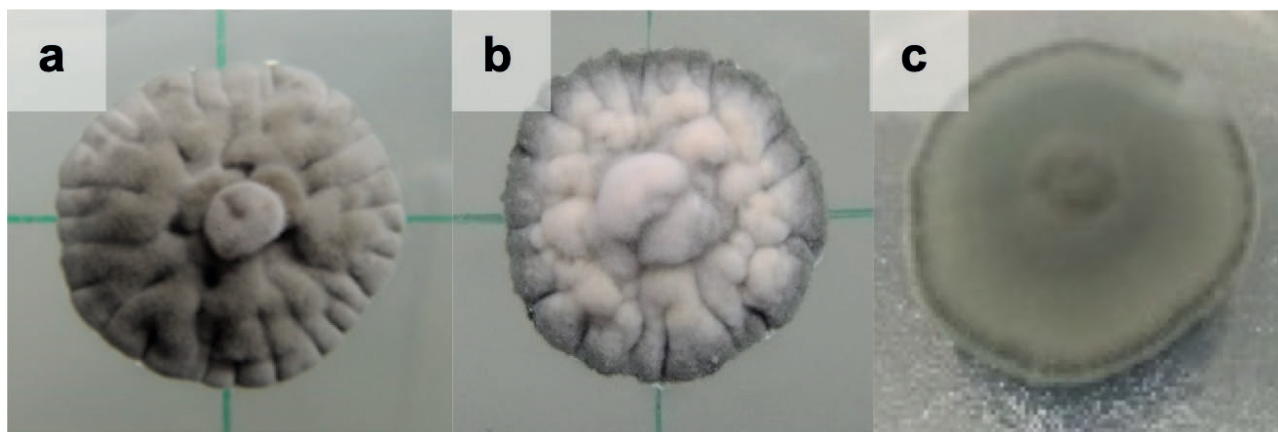


Figure 2. Morphological aspect of the tree morphotype of *Pseudocercospora cladosporioides* colonies growing in PDA culture medium during 15 days at 20°C in darkness. The three morphotypes are: a: grey and rough; b: whitish and rough and c: grey olivaceous and smooth.

Table 4. Morphological characteristics of conidia of eight representative *Pseudocercospora cladosporioides* isolates on corn meal agar.

Isolate	Colony morphology	Mean conidium dimensions (μm) ^a			Septa
		length (l)	width (w)	ratio l/w	
E19	c	101.8 \pm 3.69 a	4.4 \pm 0.10 bc	23.1 \pm 0.85 a	5.6 \pm 0.25 ab
E10	a	94.9 \pm 5.83 ab	4.9 \pm 0.15 a	19.5 \pm 1.35 abc	6.9 \pm 0.39 a
E20	a	90.1 \pm 3.69 ab	4.4 \pm 0.10 bc	20.7 \pm 0.85 ab	5.3 \pm 0.23 b
E50	a	87.1 \pm 3.69 ab	4.9 \pm 0.10 a	17.8 \pm 0.85 bc	4.8 \pm 0.25 b
E74	b	81.2 \pm 3.69 bc	4.9 \pm 0.10 a	16.7 \pm 0.85 cd	4.7 \pm 0.24 b
E33	a	80.1 \pm 3.69 bc	4.3 \pm 0.10 c	18.6 \pm 0.85 bc	4.6 \pm 0.23 bc
E71	b	75.4 \pm 3.69 bc	5.0 \pm 0.10 a	15.2 \pm 0.85 cd	4.5 \pm 0.23 bc
E12	a	65.7 \pm 3.69 c	4.9 \pm 0.10 a	13.5 \pm 0.85 d	3.6 \pm 0.24 c
Average		83.7 \pm 3.95	4.7 \pm 0.11	18.2 \pm 0.91	4.8 \pm 0.26

^a The values are means for 20 conidia, \pm standard errors. Means in a column followed by the same letter do not differ ($P = 0.05$) according to Tukey's test.

multiple folds. Four isolates were of morphotype b (Figure 2 b), which had light grey to white cottony colonies also with multiple folds. Morphotype c (five isolates; Figure 2 c) had smooth olive to grey colonies (Table 1). In all three groups, the colonies were iron-grey on the reverse sides.

Among all the total isolates examined, only eight had sparse conidium production on CMA, while none produced conidia on PDA. Presence or absence of conidia was not different between the three morphotypes. Conidia were single on each conidiophore, and were light brown. They were subcylindrical with subtruncate basal cells and obtuse apical terminal cells. The conidia ranged from 41 to 133 μm in length (mean = 83.7 μm), and from 4 to 6 μm in width (mean = 4.7 μm), and had average length to width ratio of 18.1 μm . Number of transverse septa in the conidia was from two to eight (Table 4).

Effects of temperature on mycelial growth

Based on the non-linear adjustment estimated according the generalized Analytis Beta model, the optimum mycelial growth temperature for the 41 isolates ranged from 19.2 to 24.8°C, with an average of 21.5°C. The average mycelial growth at 5°C was 0.011 mm day⁻¹, and no isolate grew at 35°C (Figure 3). Statistical analyses conducted for the ten isolates showed differences in optimal growth temperatures and maximum daily radial growth rates. Isolate E35 had the highest optimum growth temperature (24.8°C) which was greater than the other isolates, except for isolate E73 (23.9°C), while isolate E68 had the lowest optimum growth temperature (19.2°C). For daily radial growth rates at the optimum temperatures (Table 5), isolates E19 and E40 had the greatest (respectively, 0.399 and

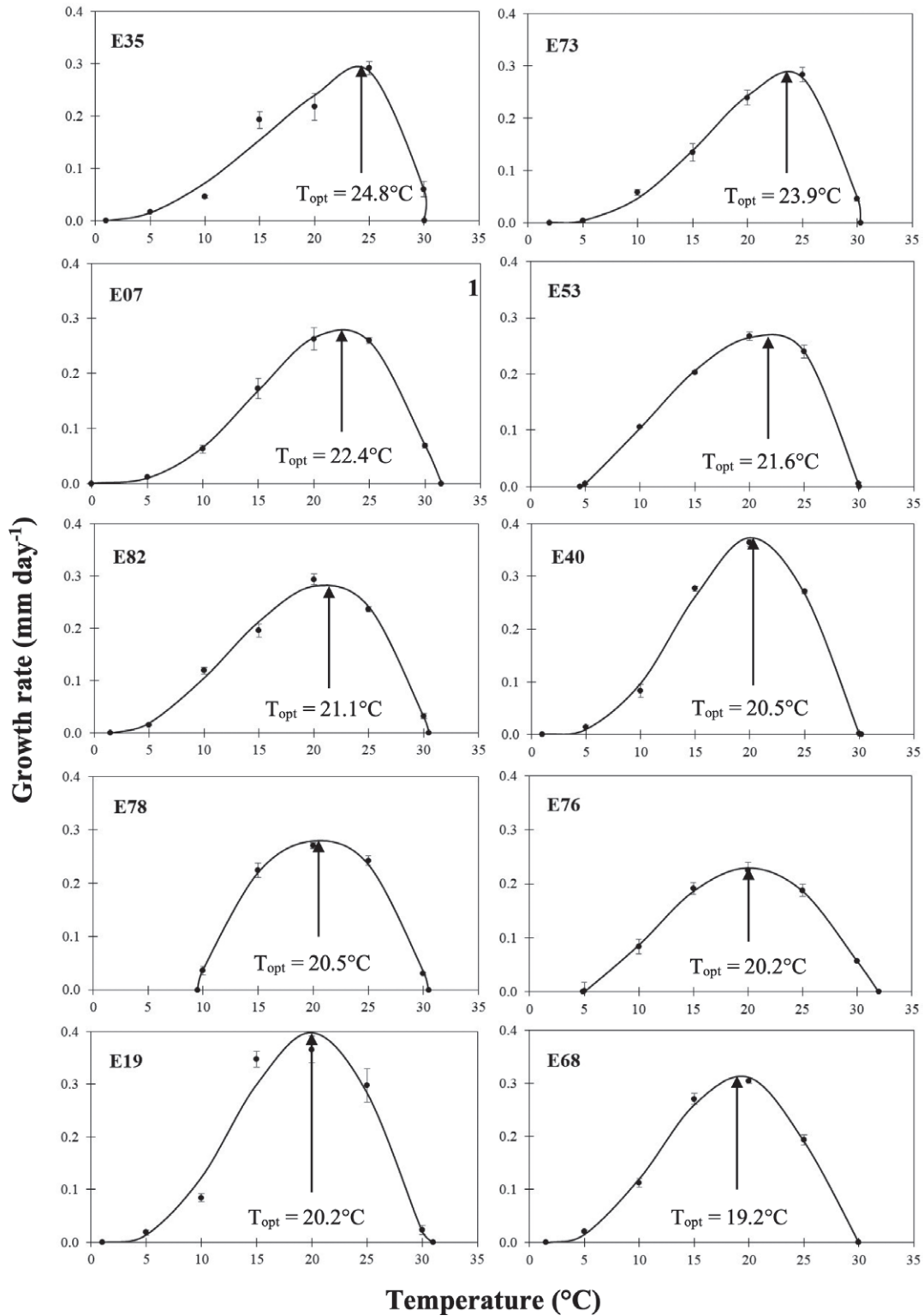


Figure 3. Effect of temperature on mycelial growth rate of a selection of ten *Pseudocercospora cladosporioides* isolates. The isolates were selected according to geographic origin, optimal growth temperature, and daily radial growth rate at the optimum temperature. Isolates were grown on PDA at 0, 5, 10, 15, 20, 25, 30 and 35°C in darkness for 30 days. For each isolate, average growth rates versus temperature were fitted to a nonlinear regression curve using the Analytis Beta model. Data points are the means of two experiments with three replicates per isolate. Vertical bars are standard errors of the mean.

Table 5. Mean temperatures and daily mycelium growth rates for ten representative isolates of ten *Pseudocercospora cladosporioides* isolates. The isolates were grown on PDA at 0, 5, 10, 15, 20, 25, 30 or 35°C in darkness for 30 d.

Isolate	Analytis Beta model ^a			Temperature (°C) ^b			Growth rate ^c (mm.day ⁻¹)
	R ²	a	b	Optimum	Minimum	Maximum	
E35	0.9570	1.98	0.42	24.8 a ^d	1.0	30.1	0.288 bc
E73	0.9969	2.69	0.79	23.9 ab	2.0	30.3	0.286 bc
E07	0.9995	3.18	1.29	22.4 bc	0.0	31.5	0.282 bc
E53	0.9998	1.37	0.69	21.6 cd	4.5	30.0	0.270 c
E82	0.9888	2.14	1.03	21.1 cde	1.5	30.5	0.285 bc
E40	0.9954	3.30	1.64	20.5 cde	3.5	30.2	0.374 a
E78	0.9968	0.82	0.74	20.5 de	9.5	30.3	0.281 bc
E76	0.9982	1.58	1.22	20.2 de	4.9	32.0	0.231 d
E19	0.9612	3.08	1.74	20.2 de	1.0	31.0	0.399 a
E68	0.9953	2.67	1.63	19.2 e	1.5	30.0	0.315 b

^a Analytis Beta model, where R² = coefficient of determination, and a and b = coefficients of regression.

^b For each isolate, temperature average growth rates were adjusted to the regression curve to optimum growth temperature.

^c Growth rates at the optimum temperature.

^d Means in each column followed by the same letter do not differ (P = 0.05), according to Tukey's test.

0.374 mm day⁻¹), while growth rate for isolate E76 was the least (0.231 mm day⁻¹).

Phylogenetic analyses

Preliminary identification based on BLAST search of ITS, ACT, and CAL gene regions, showed high similarity (99 to 100%) of all 41 isolates with the *P. cladosporioides* fungal sequences available in the GenBank Database, including the ex-epitype. The individual sequence datasets showed no significant conflicts in tree topology, indicating that the three genes could be combined. The multiple locus data matrix contained 71 taxa (41 from this study) and 933 characters, including gaps (ITS 1 - 462, ACT 463 - 655, and CAL 656 - 933), of which 75 were parsimony informative.

The tree topologies inferred from BI and ML analyses were consistent with each other. The BI trees are presented, with the support node values of both phylogenetic methods utilized (Figure 4). The 41 Uruguayan isolates grouped in a separate and robust clade (BI/ML: 1/81) with *P. cladosporioides* isolates, including the ex-epitype (CBS 117482), confirming their identity to this species.

Characterization of infection under field conditions

After 5 or 6 months from leaf inoculation, depending on whether this was conducted during autumn or spring, initial symptoms or signs of CLS became

apparent in the leaves of inoculated 'Arbequina' plants. In autumn, disease incidence in the inoculated leaves reached 86%. while in spring this reached 91%. The non-inoculated control leaves had 8% infection in both seasons (Figure 5).

Initially, the infected leaves were indistinguishable from healthy leaves. However, on the undersides of the infected leaves, distinct leaden-coloured areas began to emerge. Subsequently, yellowish and chlorotic regions appeared on the upper leaf surfaces, corresponding to the leaden underside zones. Microscopic examinations confirmed the presence of characteristic *P. cladosporioides* conidia within the leaden-grey areas on the abaxial surfaces of the inoculated leaves.

DISCUSSION

Typical CLS symptoms were observed in all of the commercial olive groves surveyed in different areas of Uruguay. This confirms that CLS is a prevalent disease in Uruguayan olive production, as previously described by Conde-Innamorato *et al.* (2013). The generally humid Uruguayan conditions and the susceptibility to CLS of the olive cultivars planted in this country probably account for this finding. Consequently, CLS can be considered as an endemic disease in Uruguay, as has been reported in Spain (Del Moral and Medina, 1985) and Italy (Nigro *et al.*, 2002).

While typical leaf spot, characterised by greenish-yellow to yellow spots with fuzzy edges on upper leaf

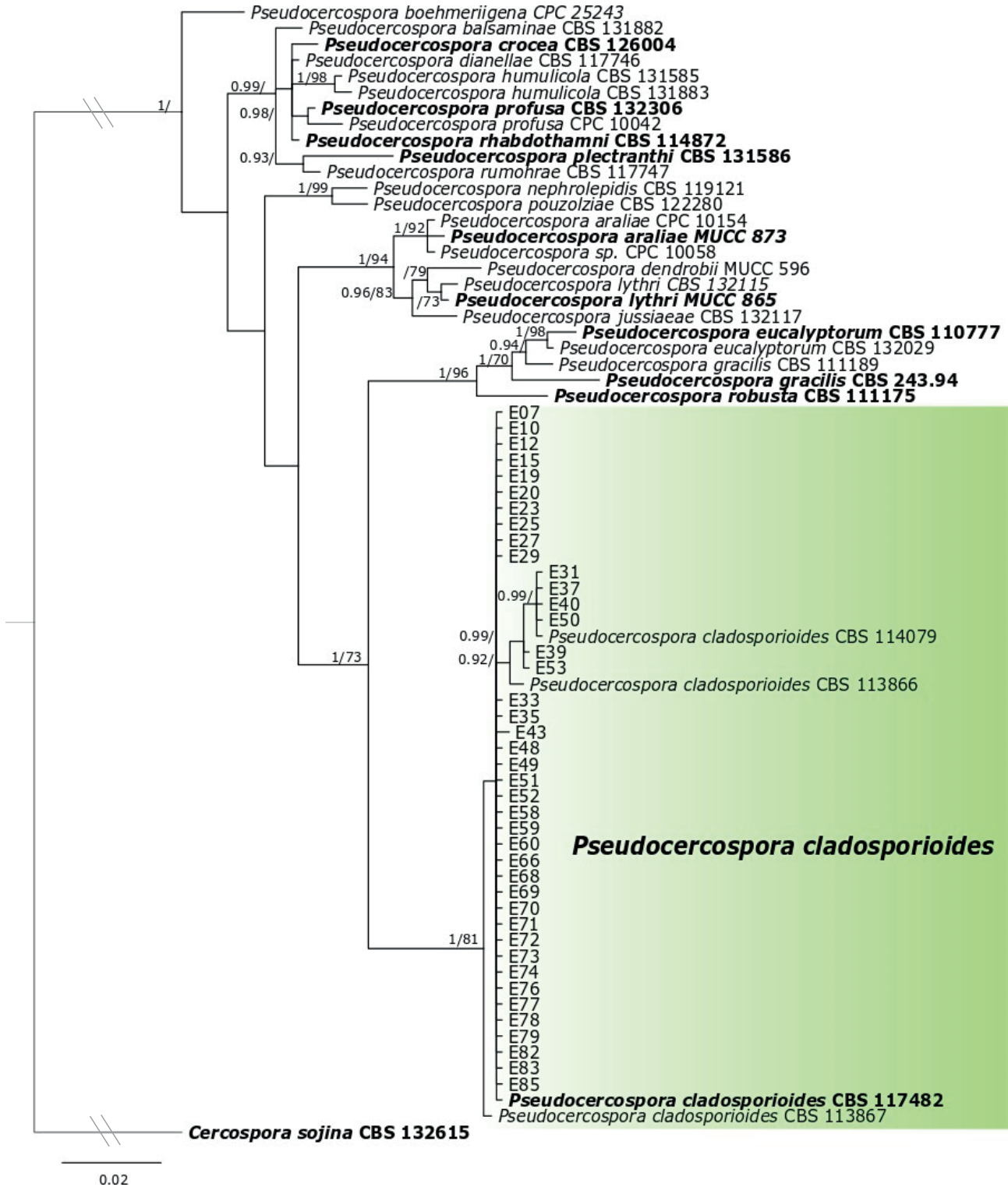


Figure 4. Bayesian inference phylogenetic tree built using the concatenated sequences of the ITS, ACT and CAL genomic regions of 41 Uruguayan isolates obtained from olive leaves with typical *Cercospora* leaf spot disease and sequences obtained from GenBank (ex-type and epi-type strains indicated in bold). *Cercospora sojina* CBS 132615 was used as an outgroup. Bootstrap support values of posterior probability (PP) and Maximum Likelihood (ML) higher than 0.90 and 70%, are shown at the nodes (PP/ML), respectively. Double hash marks indicate branch lengths shortened at least 2-fold to facilitate visualization. The scale bar represents the estimated number of substitutions per site.

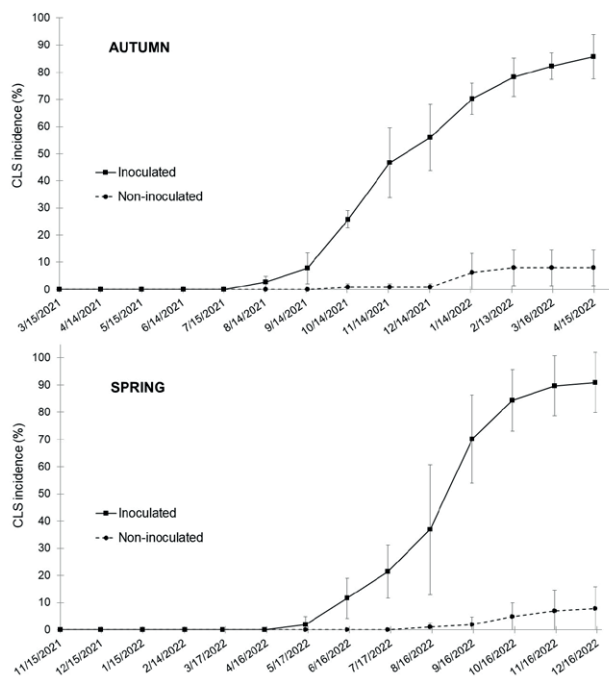


Figure 5. Development of *Cercospora* Leaf Spot symptoms in 15-year-old olive trees of the Arbequina cultivar inoculated in autumn (03/15/2021) and spring (11/15/2021) (Southern Hemisphere) with a conidial suspension of 1.5×10^5 conidia mL^{-1} of *Pseudocercospora cladosporioides* and evaluated monthly for 13 months.

surfaces, was mainly observed on older leaves (older than 8 months), this symptom was also present on young leaves (4 to 5 months), as was also documented by Nigro *et al.* (2002) and is consistent with the description of Trapero *et al.* (2017). In addition, presence of pathogen structures (*Pseudocercospora* conidia and conidiomata) was verified on the undersides of the leaves, producing leaden grey colouration. As reported by other researchers, the first pathogen signs can anticipate appearance of symptoms on the leaves (Pappas, 1993; Nigro and Ferrara, 2011), as was observed in the present study in Frantoio and Picual cultivars.

The low incidence of CLS symptoms on olive fruit has classified CLS as a foliar disease (Pappas, 1993; Abdelfattah *et al.*, 2015). However, the present study has shown that CLS symptoms on fruit were observed exclusively in one unharvested orchard 5 months after the usual olive harvest date. During autumn, the low to moderate temperatures (10–20°C) accompanied by humid and rainy periods, probably gave favourable conditions for CLS development (Giménez and Castaño, 2013; Ávila *et al.*, 2020). In addition, in Uruguay olive fruits are usually harvested early, between maturity indices of 1 and 2.5, which prioritizes oil quality over yields

(Sánchez *et al.*, 2022) and restricts CLS symptom development.

As occurs in Spain (Ávila *et al.*, 2005), the present research showed that *P. cladosporioides* was the sole causal agent of CLS in Uruguay. Multilocus phylogenetic analysis grouped the Uruguayan isolates with the ex-epitype strain of *P. cladosporioides* (CBS 117482), in a well-defined and separate clade to other *Pseudocercospora* species.

Conidium shape, size and number of transverse septae are the most important characters for morphological identification of species of *Pseudocercospora* (Ávila *et al.*, 2004). The Uruguayan isolates showed little or no sporulation on different artificial media, with only a few isolates producing a few conidia on CMA. This low or nil production of conidia in culture has been previously reported (Pappas, 1993; Avila *et al.*, 2004, 2020). In the present study, some conidia were longer than those previously reported for this species (Sarasola, 1951; Del Moral and Medina, 1985; McKenzie, 1990; Pappas, 1993; Avila *et al.*, 2004; Sergeeva *et al.*, 2008). According to Sarasola (1951), these differences can be a consequence of the origins (leaves, fruits, or artificial culture media) of the conidia. The variability of reproductive structures may also be due to the development state of conidia and to environmental conditions (Avila *et al.*, 2020). For example, Pappas (1993) mentioned that formation of large fructifications occurred in humid areas.

Optimum temperatures for mycelium growth varied for the different *P. cladosporioides* from 19.2 to 24.8°C, and maximum colony growth rate was from 0.231 to 0.399 mm day^{-1} . The optimum temperature average for the 41 isolates was 21.5°C. These parameters were similar to those reported by Avila *et al.* (2020) and Pappas (1993), who respectively reported optimum growth temperature for this fungus of 21°C and 22°C. Adaptability of the pathogen to grow in a wide range of temperatures allows it to develop in different environments.

The initial CLS symptoms on field-inoculated cv. Arbequina leaves were visible after 5 to 6 months in spring and autumn, and 11 months after the date of inoculations, infections incidence of approx. 80% was recorded. These results confirm the long incubation period of *P. cladosporioides* under field conditions (Del Moral and Medina, 1985; Trapero *et al.*, 2017; Ávila *et al.*, 2020). CLS symptoms in non-inoculated leaves can also originate from periods preceding inoculations, and these pose challenges for determining if asymptomatic leaves are healthy or are undergoing incubation periods required by this pathogen.

In conclusion, this study has confirmed the wide distribution of CLS in the olive growing regions of

Uruguay, and has indicated that *P. cladosporioides* is the causal agent of this disease in this country. Further research should prioritize comprehensive examination of the CLS disease cycle, including determination of the specific periods during which infections occur throughout each year. Additionally, understanding the evolution of inoculum production over time and developing a method to detect latent or asymptomatic infections would be valuable. Evaluating the effectiveness of fungicides for control of CLS and identifying the optimal timing for their application is also important. Assessing susceptibility or resistance of locally cultivated cultivars under specific environmental conditions is also likely to provide important knowledge to assist management of this disease.

ACKNOWLEDGMENTS

This research was funded by the Commission Sectorial the Investigation Scientific (CSIC – Uruguay). The first author obtained a scholarship from the National Agency for Research and Innovation, Uruguay (ANII scholarship POS_NAC_2017_1_141615.) to carry out the research as part of a PhD project. Dr Carlos Agustí-Brisach provided valuable collaboration relating to the use of the generalised Analytis Beta model.

AUTHOR CONTRIBUTIONS

PL was responsible for performing the assays and data analyses, and drafted the manuscript of this papers. CL, SA and PM supervised the assays, interpretation of the results, and carried out critical revisions of the manuscript. All the authors read and approved the final manuscript.

DATA AVAILABILITY STATEMENT

The dataset generated during this study are available in: <https://drive.google.com/drive/folders/1WAlgXhDEfF XaxZ1LHSdi2tPPt5NnAUXv>

LITERATURE CITED

Abdelfattah A., Li Destri Nicosia M.G., Cacciola S.O., Droby S., Schena L., 2015. Metabarcoding analysis of fungal diversity in the Phyllosphere and Carposphere of olive (*Olea europaea*). *PLoS ONE* 10: e0131069. <https://doi.org/10.1371/journal.pone.0131069>

Agustí-Brisach C., Romero J., Ávila A., Raya M.C., Roca L.F., Trapero A., 2016. Bases para la gestión integrada del emplomado del olivo. *Vida Rural*, Especial Olivar 40–48.

Ávila A., Benali A., Trapero Casas A., 2004. Variabilidad morfológica y cultural de *Pseudocercospora cladosporioides*, agente del emplomado del olivo. *Boletín de Sanidad Vegetal - Plagas* 30: 369–384. https://www.mapa.gob.es/ministerio/pags/Biblioteca/Revistas/pdf_plagas%2FBSVP-30-02-369-384.pdf

Ávila A., Groenewald J.Z., Trapero A., Crous P.W., 2005. Characterisation and epitypification of *Pseudocercospora cladosporioides*, the causal organism of Cercospora leaf spot of olives. *Mycological Research* 109(8): 881–888. <https://doi.org/10.1017/S0953756205003503>

Ávila A., Romero J., Agustí-Brisach C., Abdellatif B., Roca L.F., Trapero A., 2020. Phenotypic and pathogenic characterization of *Pseudocercospora cladosporioides*, the causal agent of Cercospora leaf spot of olives. *European Journal of Plant Pathology* 156: 45–65. <https://doi.org/10.1007/s10658-019-01861-5>

Braun U., 1993. Taxonomic notes on some species of the Cercospora complex (III). *Mycotaxon* 48: 275–298.

Carbone I., Kohn L.M., 1999. A method for designing primer sets for speciation studies in filamentous ascomycetes. *Mycologia* 91: 553–556. <https://doi.org/10.1080/00275514.1999.12061051>

Conde-Innamorato P., Montelongo M.J., Leoni C., 2013. Enfermedades del Olivo. In: *Aceites de Oliva: de la Planta al Consumidor*, Vol 1 (M.A. Grompone, J. Villamil, ed.), INIA, Montevideo, Uruguay, 183–214.

Conde-Innamorato P., Arias-Sibillotte M., Villamil J.J., Bruzzone J., Bernaschina Y., ... Leoni C., 2019. It is feasible to produce olive oil in temperate humid climate regions. *Frontiers in Plant Science* 10: 1544. <https://doi.org/10.3389/fpls.2019.01544>

Crous P.W., Braun U., Hunter G.C., Wingfield M.J., Verkley G.J.M., ... Groenewald J.Z., 2013. Phylogenetic lineages in *Pseudocercospora*. *Studies in Mycology* 75: 37–114. <https://doi.org/10.3114/sim0005>

Del Moral J., Medina D., 1985. El “repilo plomizo” del olivo causado por *Cercospora cladosporioides* Sacc., enfermedad presente en España. *Boletín de Servicio de Plagas* 11: 31–36. Available at: https://www.mapa.gob.es/ministerio/pags/Biblioteca/Revistas/pdf_plagas%2FBSVP-11-01-031-035.pdf. Accessed November 16, 2022.

Garrido A., Fernández-González M., Cortiñas Rodríguez J.A., Carrera L., González-Fernández E., ... Rodríguez-Rajo F.J., 2022. Fungal phytopathogenic spore first assessment in an olive orchard of Northwestern Spain. *Agronomy* 12: 246. <https://doi.org/10.3390/agronomy12020246>

- Giménez A., Castaño J.P., 2013. Características agroclimáticas del Uruguay. In: *Aceites de Oliva: de la Planta al Consumidor*, Vol 1 (M.A. Grompone, J. Vilamil, ed.), INIA, Montevideo, Uruguay, pp. 37–50.
- Hau B., Kranz J. 1990. Mathematics and statistics for analyses in epidemiology. In: *Epidemics of Plant Diseases* (J. Kranz, ed.), Springer International Publishing, Berlin, Germany, 12–52.
- López-Moral A., Raya-Ortega M.C., Agustí-Brisach C., Roca L.F., Lovera M., ... Trapero A. 2017. Morphological, pathogenic, and molecular characterization of *Colletotrichum acutatum* isolates causing almond anthracnose in Spain. *Plant Disease* 101: 2034–2045. <https://doi.org/10.1094/PDIS-03-07-0318-RE>
- McKenzie E.H.C., 1990. New plant disease records in New Zealand: Miscellaneous fungal pathogens II. *New Zealand Journal of Crop and Horticultural Science* 18: 65–73. <https://doi.org/10.1080/01140671.1990.10428073>
- MGAP-DIEA, 2020. Censo de productores de olivos 2020. Serie Trabajos Especiales 364: 46. Available at: https://www.gub.uy/ministerio-ganaderia-agricultura-pesca/sites/ministerio-ganaderia-agricultura-pesca/files/2021-03/PUBLICACION_Olivos2020_Final.pdf. Accessed November 16, 2022.
- Nigro F., Ferrara M., 2011. Olive cercosporiosis. In: *Olive Diseases and Disorders* (L. Scherna, G.E. Agosteo, S.O. Cacciola, ed.), India Transworld Research Network, 247–258.
- Nigro F., Ippolito A., Gallone P., Romanazzi G., Carmignano P., Laccone G., 2002. Cercosporiosis of olive in Apulia and Attempts to control the disease. *Acta Horticulturae* 586: 773–776. <https://doi.org/10.17660/ActaHortic.2002.586.167>
- Paolocci F., Rubini A., Granetti B., Arcioni S., 1999. Rapid molecular approach for reliable identification of *Tuber* spp. ectomycorrhizae. *FEMS Microbiology Ecology* 28: 23–30. <https://doi.org/10.1111/j.1574-6941.1999.tb00557.x>
- Pappas A.C., 1993. *Mycocentrospora cladosporioides* on olive in Greece. *Bulletin OEPP/EPPO* 23: 405–409 <https://doi.org/10.1111/j.1365-2338.1993.tb01344.x>
- Romero J., Ávila A., Agustí-Brisach C., Roca L.F., Trapero A., 2020. Evaluation of fungicides and management strategies against cercospora leaf spot of olive Caused by *Pseudocercospora cladosporioides*. *Agronomy* 10: 271. <https://doi.org/10.3390/agronomy10020271>
- RStudio v. 2023.06.1-524 (<https://dailies.rstudio.com/version/2023.06.1+524/>).
- Sánchez B., Mastrogiovanni M., Santos M., Petingi S., Conde-Innamorato P., ... Rubbo H., 2022. Detection of nitro-conjugated linoleic acid and nitro-oleic acid in virgin olive oil under gastric conditions: relationship to cultivar, fruit ripening, and polyphenol content. *ACS Food Science & Technology* 2: 673–681. <https://doi.org/10.1021/acsfoodscitech.1c00477>
- Sarasola A.A., 1951. A new disease of Olive in Argentina caused by *Cercospora cladosporioides* Sacc. *Revista de la Facultad de Agronomía*, Universidad Nacional de La Plata 28: 41–47.
- Sergeeva V., Braun U., Spooner-Hart R., Nair N., 2008. First report of *Pseudocercospora cladosporioides* on olive (*Olea europaea*) berries in Australia. *Australasian Plant Disease Notes* 3: 24. <https://doi.org/10.1071/DN08010>
- Sergeeva V., Spooner-Hart R., 2009. Anthracnose and Cercosporiose on olives in Australia: an update. *Australian & New Zealand Olivegrower and Processor* 65: 31–34. Available at: https://olivediseases.com/wp-content/uploads/2015/02/vera_anthracnosecercosporiose.pdf Accessed November 16, 2022
- Tamura K., Stecher G., Kumar S., 2021. MEGA11: molecular evolutionary genetics analysis version 11. *Molecular Biology and Evolution* 38: 3022–3027.
- Trapero A., López F.J., Blanco M.A., 2017. Enfermedades. In: *El Cultivo del Olivo*. (D. Barranco, R. Fernández-Escobar, L. Rallo, ed.), Mundi-Prensa, Madrid, Spain, 733–798.
- White T.J., Bruns T.D., Lee S., Taylor J.W., 1990. Amplification and direct sequencing of fungal ribosomal RNA genes for phylogenetics. In: *PCR protocols- A guide to methods and applications* (M.A. Innes, D.H. Gelfand, J.J. Sninsky, T.J. White, ed.), Academic Press, London, UK, 315–322.